Noncoherent and Coded OFDM Using Decision–Feedback Demodulation and Diversity

Lutz H.–J. Lampe[1], Robert Schober, Robert F.H. Fischer

Laboratorium für Nachrichtentechnik, Universität Erlangen–Nürnberg
Cauerstraße 7/NT, D–91058 Erlangen, Germany

Phone: +49-9131-85-28718, Fax: +49-9131-85-28919, Email: LLampe@LNT.de

I. Introduction

Multi–carrier techniques are an attractive alternative to single–carrier systems when transmitting over frequency–selective channels. For example, orthogonal frequency–division multiplexing (OFDM) for digital audio broadcasting [1], digital video broadcasting [2], and HIPERLAN [3] are successfully proposed and standardized multi–carrier transmission systems in Europe. The American National Standardization Institute has selected discrete multitone (DMT) transmission for asymmetric digital subscriber lines [4]. Currently, OFDM is discussed as modulation scheme for power–line communications providing high–speed network access, e.g. [5].

The main advantage of multi–carrier transmission compared to single–carrier systems is the low complexity of channel equalization, which is even more manifest if differential encoding and noncoherent detection are applied. Then, explicit channel estimation, which usually is based on pilot symbols, and equalization can be circumvented. Generally, the price to be paid for robust and low complex noncoherent detection is a performance loss against coherent receivers, which strongly depends on the characteristics of the underlying transmission channel.

In this paper, we concentrate on OFDM schemes, where OFDM symbols consecutive in time are supposed to be *separately* detected. This is for example necessary in multi–user systems applying time–division multiple access. To utilize *diversity* channel coding in combination with bit–interleaving across the OFDM subcarriers is regarded. A good trade–off between coding gain and complexity is given by convolutional codes and maximum–likelihood decoding with the Viterbi algorithm. We will consider the possibility of using a further degree of diversity by transmitting the coded information over several independent fading channels, which in a practical system can be achieved e.g. by frequency hopping or multiple–antenna receivers. This becomes necessary if unfavorable short–time fading conditions lead to severe performance degradation. Since for the described situation coherent detection requires pilot symbols for channel estimation in *each* OFDM symbol, the overhead for coherent receivers can be regarded as prohibitive. Hence, reception without channel state information is recommendable.

For the scenario explained above we adopt a simple receiver structure proposed in [6], [7]. There, power efficiency of noncoherent M–ary differentially encoded phase–shift keying (MDPSK) transmission over flat Rayleigh fading channels is considerably increased by enlarging the observation interval of noncoherent reception to $N > 2$. Specifically, *hard* decisions of the Viterbi algorithm are fed back in an iterative decoding procedure. This decision–feedback differential demodulation (DF–DM) can be regarded as analogous to decision–feedback differential detection (DF–DD) for uncoded transmission [8], [9]. Though hard decision feedback is clearly suboptimum, it has shown sufficient rate of convergence and substantial performance gains with only a very moderate increase in complexity compared to conventional differential detection with $N = 2$ [6], [7]. Noteworthy, there are a number of other known iterative decoding schemes for MDPSK transmission, e.g. [10], [11], [12], [13]. There, however, computational complexity increases exponentially with N.

In this contribution, we extend the approach of [6], [7] to OFDM over frequency–selective fading channels. Whereas in [6], [7] high diversity has been achieved by sufficient bit–interleaving, for OFDM this strategy is only partly suitable. Instead, we quantify the influence of different degrees of diversity on system performance. First, the transmission model is introduced. Then, the metric calculation for DF–DM and the iterative decoding algorithm are given. For evaluation of the proposed noncoherent receiver simulation results of OFDM with parameters according to established systems [1], [2], [3] are discussed.

II. System Model

We regard transmission over time–variant frequency–selective channels. First, coding and interleaving are performed within only one OFDM symbol. The block diagram of the discrete–time system model in the equivalent low–pass domain is depicted in Figure 1.

[1] Corresponding Author

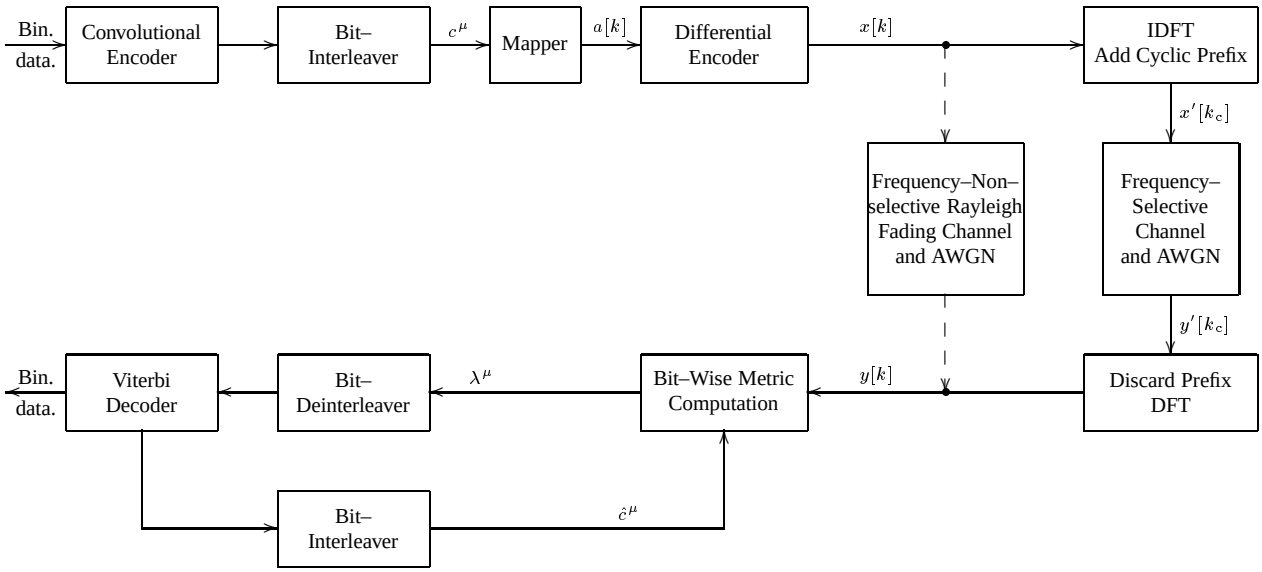

Fig. 1. Discrete–time system model.

The discrete–time impulse response $h[\nu]$, $0 \leq \nu \leq L-1$, is modeled as an FIR filter of length L. As for many applications we assume statistically independent zero–mean complex Gaussian distributed impulse response coefficients with variances $\sigma^2_{h[\nu]}$ according to a given channel power–delay profile, cf. e.g. [14]. The coefficients are assumed to be constant during one OFDM symbol, which consists of D subcarriers.

The convolutional encoder output symbols are bit–wise interleaved, and $\ell \triangleq \log_2(M)$ interleaved coded bits c^μ, $0 \leq \mu \leq \ell - 1$, are mapped ($\mathcal{M}(\cdot)$) to M–ary PSK symbols $a[k]$ ($k \in \mathbb{Z}$: discrete–time data symbol index). This bit–interleaved coded modulation (BICM) has been proved to be very effective for Rayleigh fading channels [15], [16]. In order to enable noncoherent demodulation for each OFDM symbol, blocks of $D-1$ symbols $a[k]$ are differentially encoded to give D absolute symbols $x[k]$, i.e., $x[k] = a[k] \cdot x[k-1]$, where the first $x[k]$ of each block serves as a reference symbol. Via IDFT ((I)DFT: (inverse) discrete Fourier transform) these blocks are transformed into transmit symbols $x'[k_c]$ ($k_c \in \mathbb{Z}$: discrete–time transmit symbol index). Each block of D transmit symbols is prefixed with the D_0 last samples, the so–called guard interval [17], of the same block at the transmitter, and D out of $D + D_0$ received symbols $y'[k_c]$ are used for further processing. Thereby, if the length D_0 of the guard interval is chosen such that $D_0 \geq L-1$, the linear convolution of transmitted signal and channel impulse response is converted into a cyclic convolution. Subsequently, we always assume that $D_0 \geq L-1$ holds. The IDFT/DFT pair of OFDM resolves this cyclic convolution such that the transmission between the IDFT input and the DFT output is performed in D parallel, independent subchannels. For coding across these subchannels, a frequency–nonselective (flat) fading channel between $x[k]$ and $y[k]$ (cf. Figure 1), with complex fading gains $g[k]$ equal to the samples of the underlying channel transfer function is obtained:

$$y[k] = g[k] \cdot x[k] + n[k] \,, \tag{1}$$

where $n[k]$ denotes independent additive white Gaussian noise (AWGN).

By virtue of the DFT the fading gains $g[k]$ are correlated, zero–mean complex Gaussian random variables. The autocorrelation function of the fading process is given by ($\mathcal{E}$ denotes expectation)

$$\begin{aligned} R_g[\kappa] &\triangleq \mathcal{E}\{g[k+\kappa]g^*[k]\} \\ &= \mathcal{E}\left\{ \sum_{\nu_1=0}^{L-1} h[\nu_1] \mathrm{e}^{-\mathrm{j}\frac{2\pi}{D}\nu_1(k+\kappa)} \sum_{\nu_2=0}^{L-1} h^*[\nu_2] \mathrm{e}^{\mathrm{j}\frac{2\pi}{D}\nu_2 k} \right\} \\ &= \sum_{\nu=0}^{L-1} \sigma^2_{h[\nu]} \mathrm{e}^{-\mathrm{j}\frac{2\pi}{D}\nu\kappa} \,, \end{aligned} \tag{2}$$

which is the DFT of the power–delay profile.

At the receiver, bit branch metrics λ^μ are computed based on an extended observation interval of $N > 2$ symbols as described in Section III. The deinterleaved metrics are the soft input for the standard Viterbi decoder. The *hard* decisions of the Viterbi decoder are interleaved and fed back to the metric calculation (cf. Figure 1) which now makes use of the decisions $\hat{c}^\mu$. This procedure is repeated in a number of iterations.

So far, in the above scheme diversity is achieved by coding across OFDM subcarriers. However, depending on channel characteristics, transmission bandwidth, and number of OFDM subcarriers there might be situations, where this frequency diversity is not sufficient, e.g. if the equivalent flat fading channel of OFDM resembles a block fading channel. Then, to counter

the effects of unfavorable fading realizations on the overall performance, diversity has to be improved by coding across different channel realizations (cf. e.g. [18] for the case of block fading). That is, coding and interleaving are performed over a number of d OFDM symbols, which are transmitted over independent fading channels, e.g. by implementing frequency hopping techniques or multiple–antenna systems.

III. Metric Calculation

The noncoherent metric computation should incorporate the dependences between consecutive channel output symbols (see (2)) as completely as possible. Consequently, branch metric λ^μ is obtained using the complex N–dimensional probability density function (pdf) $p(\boldsymbol{y}[k]|\boldsymbol{a}[k])$ of $\boldsymbol{y}[k] \triangleq [y[k], y[k-1], \ldots, y[k-N+1]]^T$ under the assumption $\boldsymbol{a}[k] \triangleq [a[k], a[k-1], \ldots, a[k-N+2]]^T$, i.e, we base the metric on the observation of N received symbols. Here, observations $\boldsymbol{y}[k]$ are overlapping by $N-1$ symbols (sliding window). The pdf $p(\boldsymbol{y}[k]|\boldsymbol{a}[k])$ is derived e.g. in [19] for the flat Rayleigh fading channel.

Optimally, M^{N-1} pdfs for all possible vectors $\boldsymbol{a}[k]$ have to be determined for the ℓ address bits which label the scalar symbol $a[k]$. Then, M^{N-1}/ℓ pdf calculations per bit metric are necessary, i.e., the computational effort grows exponentially with the observation length N. Instead of considering all vector symbols $\boldsymbol{a}[k]$, we substitute hard decision–feedback symbols $\hat{a}[k-\nu]$, $1 \leq \nu \leq N-2$, which considerably reduces the computational effort (cf. also [9]). The generation of feedback symbols is described in Section IV.

The metric computation is further simplified if also $\ell - 1$ decision–feedback address bits $\hat{c}^\mu$ of $a[k]$ are fed back. Doing this, only $\ell + 1 < M$ pdfs have to be determined since only $\ell + 1$ different $a[k]$ are possible. Neglecting all terms in the pdfs which do not depend on the symbol $a[k]$, the resulting bit metric for bit b at labeling position μ is simply given by [9]

$$\lambda_b^\mu = \mathrm{Re}\left\{ \tilde{a}[k] y^*[k] \cdot \sum_{\nu=1}^{N-1} t_{0\nu} y[k-\nu] \prod_{n=1}^{\nu-1} \hat{a}[k-n] \right\}, \quad (3)$$

where $b \in \{0,1\}$ and the trial symbol $\tilde{a}[k] = \mathcal{M}(\hat{c}^0, \ldots, \hat{c}^{\mu-1}, b, \hat{c}^{\mu+1}, \ldots, \hat{c}^{\ell-1})$ are used. $t_{0\nu}$, $1 \leq \nu \leq N-1$, is determined by the statistics of the fading process and is defined in [9, Eq. (15)]. Figure 2 illustrates the composition of vector $\boldsymbol{a}[k]$ for the decision–feedback based metric computation.

Since a positive multiplicative constant is of no importance for the decoding decisions in the Viterbi algorithm, it is possible to replace $t_{0\nu}$ by $p_{0\nu} \triangleq c_0 \cdot t_{0\nu}$, $c_0 \in \mathbb{R}^+$, $\nu = 1, 2, \ldots, N-1$. If c_0 is chosen properly (cf. [9]), $p_{0\nu}$ are the coefficients of a linear $(N-1)$st order minimum mean–squared error (MMSE) FIR predictor for the random process $g[\cdot] + n[\cdot]x^*[\cdot]$. In this case, these coefficients $p_{0\nu}$ can be adaptively determined in a simple manner by employing, e.g. the recursive least–squares (RLS) algorithm [20].

Noteworthy, the number of branch bit metrics λ_b^μ is independent of the observation length N, and identical to that of conventional differential demodulation with $N = 2$ and without feedback.

IV. Iterative Decoding Algorithm

For DF–DD of uncoded MDPSK the feedback symbols $\hat{a}[k-\nu]$ stem from immediate decisions on transmitted symbols [8], [9]. When error correction coding and bit–interleaving are applied it is reasonable to obtain the decision–feedback symbols from the bit decisions $\hat{c}^\mu$ of the Viterbi decoder via remodulation. Of course, for the first demodulation of a received sequence (first decoding iteration), no previous decisions $\hat{c}^\mu$ are available. Then, in order to keep the demodulation as simple as possible, we resort to conventional differential demodulation based on two consecutive received symbols and without feedback. For the further demodulation operations (decoding iterations) remodulated feedback symbols $\hat{a}[k-\nu]$ and address bits $\hat{c}^\mu$ are used in order to calculate bit branch metrics based on an observation interval $N > 2$ (cf. Eq. (3)).

Since the algorithm has an iterative structure the question of convergence arises. Assuming ideal interleaving, i.e., sufficient diversity such that feedback bits (symbols) are virtually mutually independent and independent of the corresponding channel gain, and regarding the demodulation with observation length $N > 2$ as an estimation problem it is shown in [7] that the algorithm converges for usually desired bit error rates (BER). If insufficient diversity does not justify an ideal interleaving assumption it is expected that the rate of convergence deteriorates due to correlated feedback (see Section V).

V. Simulation Results and Discussion

In order to assess the proposed demodulation technique, computer simulations of the system in Figure 1 have been performed. As interesting scenarios, OFDM with $D = 1024$ subcarriers over frequency–selective Rayleigh fading channels with the "hilly terrain" power–delay profile according to COST 207 and OFDM with $D = 64$ and an exponentially decreasing power–delay profile with $\ln(\sigma^2_{h[\nu]}/\sigma^2_{h[\nu-1]}) = 0.5$, $1 \leq \nu \leq L-1$, $L = 16$, have been considered. The parameters of the first scenario are typical for digital broadcasting or mobile communication systems (cf. e.g. [1], [2], [21]), the second parameter set is more suited to wireless local area networks (cf. e.g. [3]). The fading channel is assumed to remain constant during the transmission of one OFDM symbol. To model the effect of channel diversity, coding and bit–interleaving are done across d OFDM

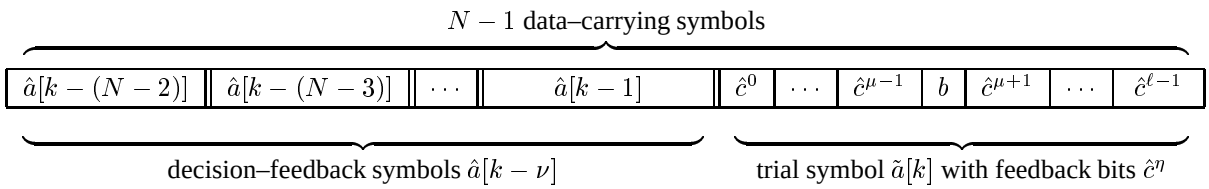

Fig. 2. Composition of vector $\boldsymbol{a}[k]$ for decision–feedback based computation of λ_b^μ.

symbols, which are transmitted over d independent fading channels.

As coded modulation schemes, BICM and 4DPSK with the standard rate 1/2 convolutional code with 64 states (generator polynomials $(133, 171)_8$) and more bandwidth efficient 8DPSK with a punctured rate 2/3 convolutional code with 64 states (generator polynomials $(135, 163)_8$) are employed. Usual Gray labeling [16] and randomly generated bit–interleavers are applied.

For the sake of clarity, subsequently simulation results for DF–DM after four iterations are plotted only. However, it should be noted that in most cases almost identical BERs are obtained with only two iterations.

First, the simulation results for OFDM with $D = 1024$ and the "hilly terrain" power–delay profile are discussed. Figures 3 and 4 present the measured BERs as functions of $\bar{E}_b/N_0$ ($\bar{E}_b$: average received energy per information bit, N_0: one–sided noise power spectral density) for 4DPSK, extended observation intervals $N = 3, 5$, and diversity $d = 1, 2, 6$. As performance limits, the BERs for genie–aided DF–DM, i.e., all decision–feedback symbols are correct, are plotted.

For diversity $d = 1$, i.e., each OFDM symbol is independently processed (Figure 3), iterative DF–DM with $N = 3$ leads to a gain of about 0.8 dB at $\mathrm{BER} \approx 10^{-4}$ over conventional demodulation with $N = 2$. The promised gain of 1 dB for genie–aided feedback is almost achieved. However, for $N = 5$ convergence is significantly slower than for $N = 3$. At $\mathrm{BER} \approx 10^{-4}$ a gap of about 0.6 dB between real and genie–aided feedback remains. Thus, here DF–DM with $N = 5$ is attractive only for $\mathrm{BER} < 10^{-4}$.

When diversity is increased to $d = 2$ or 6 (Figure 4) the performance considerably improves in general. This indicates that in case of $d = 1$ performance is severely affected by variations of short–term channel characteristics, e.g. fluctuations in received power. Iterative DF–DM benefits even more from enhanced diversity than standard noncoherent demodulation. For $d = 6$, the curves of DF–DM with $N = 3, 5$ are practically converged to the corresponding curves of genie–aided DF–DM at $\mathrm{BER} \approx 10^{-4}$, and gains of about 1.2 dB with $N = 3$ and 1.7 dB with $N = 5$, respectively, are achieved. Noteworthy, these gains can be precisely predicted by a theoretical analysis of the associated cutoff rate for genie–aided DF–DM, where the effective fading channel is assumed to be ergodic [7].

To further point out the potential of the proposed receiver structure, Figure 5 gives the block error rate (BLER) for the above setup with $d = 1$. As can be seen from Figure 5 when regarding BLER iterative DF–DM is superior to conventional demodulation by about 1.0–1.5 dB in power efficiency. Moreover, BLER always improves for increasing N, i.e., iterative DF–DM converges quickly.

The simulation results for 8DPSK are depicted in Figure 6. Here, similar conclusions as for 4DPSK can be drawn. By iterative DF–DM with $N = 3$ gains of 0.5 dB, 1.0 dB, and 1.1 dB for diversity of $d = 1$, $d = 2$, and $d = 6$, respectively, are obtained. DF–DM with $N = 5$, which is not shown in Figure 6, does not yield improvements compared to $N = 3$. Remarkably, this coincides with the results of the cutoff rate analysis, which reveals that achievable gains depend on the desired modulation rate (cf. [7]).

Next, the transmission scenario for OFDM with $D = 64$ subcarriers is regarded. In Figures 7 and 8, the simulation results for conventional demodulation with $N = 2$ and iterative DF–DM with $N = 3, 5$ are compared for diversity $d = 1$ and $d = 2, 6$, respectively. Obviously, for $d = 1$ (Figure 7) a flattening of the BER curves occurs. Due to the relatively short channel impulse response and the low number of subcarriers the adverse effects of channel variations over OFDM symbols are more pronounced. Iterative DF–DM can partly remove the flattening, but the curves of DF–DM and genie–aided DF–DM diverge. The situation changes if further diversity is introduced, i.e., $d = 2, 6$ (Figure 8). Whereas for demodulation with $N = 2$ a flattening remains, with DF–DM flattening of the BER curves vanishes. Again, the higher the degree of diversity the faster iterative DF–DM converges. Altogether, for this scenario immense gains of several dB in power efficiency are obtained with DF–DM.

VI. Conclusions

Noncoherent OFDM transmission over slowly time–variant frequency–selective channels is considered. We have investigated the application of a simple iterative receiver structure, which has proved to offer considerable performance gains with only very moderate increase in complexity compared to standard noncoherent reception. Also the effects of diversity on power efficiency and convergence are examined.

Based on transmission scenarios of high practical relevance

it is shown that iterative DF–DM is a promising alternative to conventional differential demodulation. For all situations, DF–DM can improve the performance of noncoherent OFDM. Especially if sufficient channel diversity is provided, iterative DF–DM shows good convergence and leads to significant gains in power efficiency. Since for DF–DM metric computation is simple and gains are achieved after only a few iterations, in many cases two iterations are sufficient, computational complexity remains low.

Noteworthy, the proposed noncoherent demodulation technique is also applicable to transmission schemes, where frames of consecutive OFDM symbols are jointly processed. Then, a two–dimensional approach exploiting correlation both in time and in frequency has to be chosen, similar to the one described in [22] for uncoded pilot symbol assisted detection. The analysis of the resulting scheme is a topic of current research.

REFERENCES

[1] European Telecommunications Standards Institute (ETSI). Radio broadcasting systems; Digital Audio Broadcasting (DAB) to mobile, portable and fixed receivers. ETS 300 401, May 1997.

[2] European Telecommunications Standards Institute (ETSI). Digital Video Broadcasting (DVB); Framing structure, channel coding and modulation for digital terrestrial television. ETSI EN 300 744, July 1999.

[3] European Telecommunications Standards Institute (ETSI). Broadband Radio Access Networks (BRAN); HIPERLAN Type 2; Physical layer. ETSI TS 101 475, April 2000.

[4] American National Standards Institute (ANSI). Asymmetric Digital Subscriber Line (ADSL) Metallic Interface. Draft American National Standard for Telecommunications, 1998.

[5] L.H.-J. Lampe and J.B. Huber. Bandwidth Efficient Power Line Communications Based on OFDM. *Archiv für Elektronik und Übertragungstechnik (International Journal of Electronics)*, 54(1):2–12, 2000.

[6] L.H.-J. Lampe and R. Schober. Decision–Feedback Differential Demodulation of bit–interleaved coded MDPSK. *Electronics Letters*, 35(25):2170–2171, December 1999.

[7] L.H.-J. Lampe and R. Schober. Iterative Decision–Feedback Differential Demodulation of Bit–Interleaved Coded MDPSK for Flat Rayleigh Fading Channels. *In revision: IEEE Trans. Com., 1999*.

[8] F. Adachi and M. Sawahashi. Decision Feedback Multiple–Symbol Differential Detection of M–ary DPSK. *Electronics Letters*, 29(15):1385–1387, July 1993.

[9] R. Schober, W.H. Gerstacker, and J.B. Huber. Decision–Feedback Differential Detection of MDPSK for Flat Rayleigh Fading Channels. *IEEE Trans. on Com.*, 47(7):1025–1035, July 1999.

[10] M. Peleg and S. Shamai (Shitz). Iterative Decoding of Coded and Interleaved Noncoherent Multiple Symbol Detected DPSK. *Electronics Letters*, 33(12):1018–1020, June 1997.

[11] T. May and H. Rohling. Zur Detektion differentieller Modulation in codierten OFDM-Systemen. In *3. OFDM-Fachgespräch*, Braunschweig, September 1998.

[12] P. Hoeher and J. Lodge. "Turbo DPSK": Iterative Differential PSK Demodulation and Channel Decoding. *IEEE Trans. on Com.*, 47(6):837–843, June 1999.

[13] I. D. Marsland and P. T. Mathiopoulos. On the Performance of Iterative Noncoherent Detection of Coded M–PSK Signals. *IEEE Trans. on Com.*, 48(4):588–596, April 2000.

[14] B. Sklar. Rayleigh Fading Channels in Mobile Digital Communication Systems—Part I: Characterization. *IEEE Com. Magazin*, 35(7):90–101, July 1997.

[15] E. Zehavi. 8–PSK Trellis Codes for a Rayleigh Channel. *IEEE Trans. on Com.*, 40(5):873–884, May 1992.

[16] G. Caire, G. Taricco, and E. Biglieri. Bit–Interleaved Coded Modulation. *IEEE Trans. on Inf. Theory*, 44(3):927–946, May 1998.

[17] J.A.C. Bingham. Multicarrier Modulation for Data Transmission: An Idea Whose Time Has Come. *IEEE Communications Magazine*, pages 5–14, May 1990.

[18] R. Knopp and P.A. Humblet. On Coding for Block Fading Channels. *IEEE Trans. on Inf. Theory*, 46(1):189–205, January 2000.

[19] P. Ho and D. Fung. Error Performance of Multiple–Symbol Differential Detection of PSK Signals Transmitted over Correlated Rayleigh Fading Channels. *IEEE Trans. on Com.*, 40:25–29, October 1992.

[20] R. Schober and W.H. Gerstacker. Decision-Feedback Differential Detection Based on Linear Prediction for MDPSK Signals Transmitted Over Ricean Fading Channels. *IEEE J. Select. Areas Commun.*, March 2000.

[21] T. May, H. Rohling, and V. Engels. Performance Analysis of Viterbi Decoding for 64–DAPSK and 64–QAM Modulated OFDM Signals. *IEEE Trans. on Com.*, 46(2):182–190, February 1998.

[22] P.K. Frenger and N.A.B. Svensson. Decision–Directed Coherent Detection in Multicarrier Systems on Rayleigh Fading Channels. *IEEE Trans. Vehicular Technology*, 48(2):490–498, March 1999.

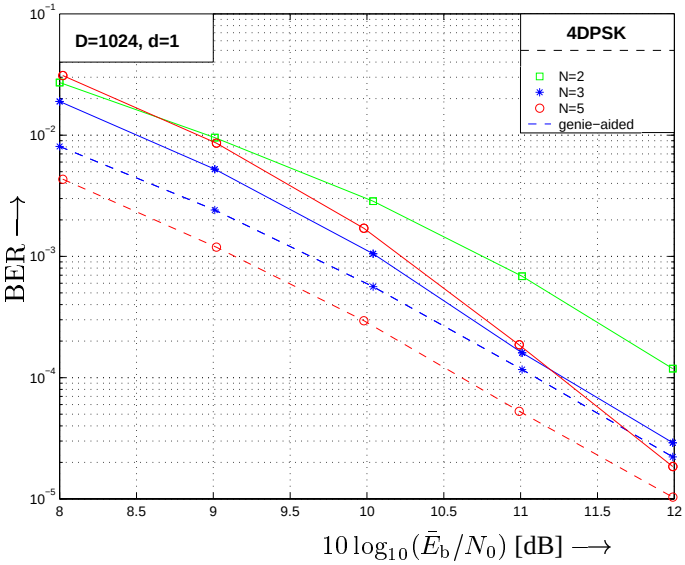

Fig. 3. BER over $10\log_{10}(\bar{E}_b/N_0)$. OFDM with $D = 1024$, 4DPSK, and diversity $d = 1$ (independent processing of each OFDM symbol). Conventional differential demodulation with $N = 2$. Iterative DF–DM with $N = 3, 5$ after four iterations.

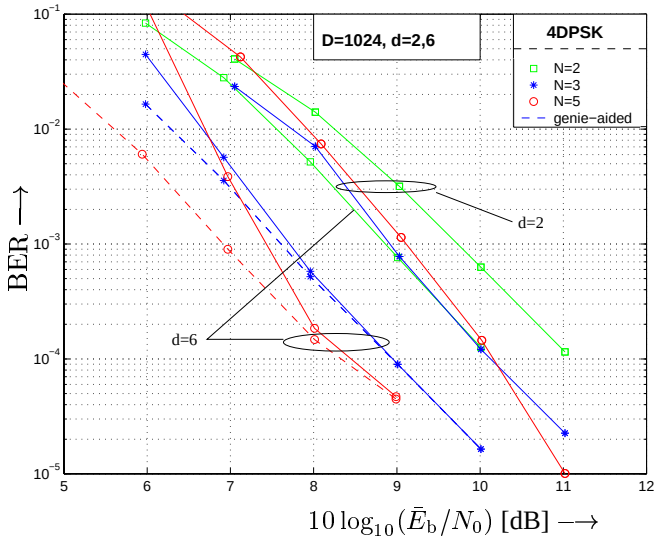

Fig. 4. BER over $10\log_{10}(\bar{E}_b/N_0)$. OFDM with $D = 1024$, 4DPSK, and diversity $d = 2, 6$. Conventional differential demodulation with $N = 2$. Iterative DF–DM with $N = 3, 5$ after four iterations.

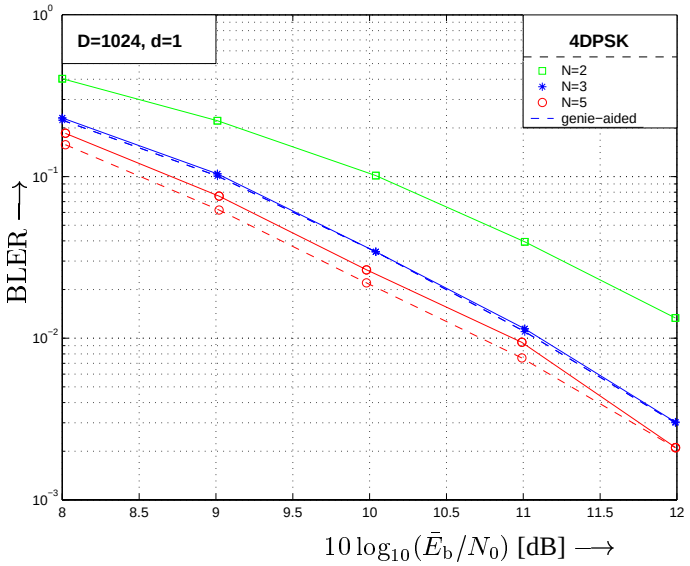

Fig. 5. BLER over $10\log_{10}(\bar{E}_b/N_0)$. OFDM with $D = 1024$, 4DPSK, and diversity $d = 1$ (independent processing of each OFDM symbol). Conventional differential demodulation with $N = 2$. Iterative DF–DM with $N = 3, 5$ after four iterations.

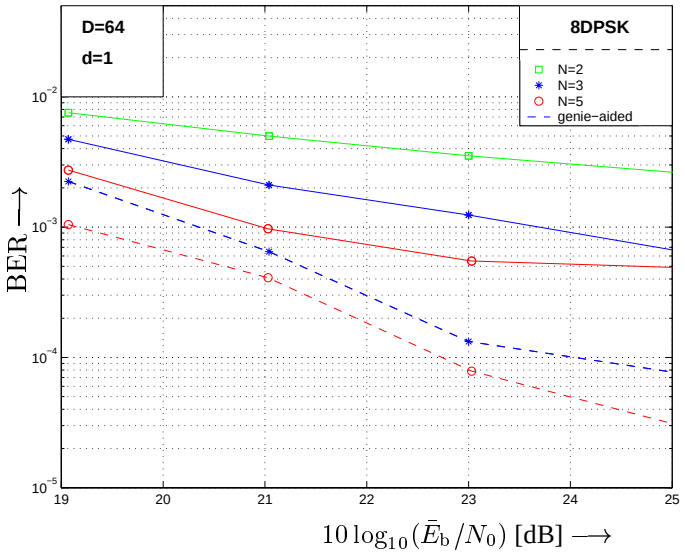

Fig. 7. BER over $10\log_{10}(\bar{E}_b/N_0)$. OFDM with $D = 64$, 8DPSK, and diversity $d = 1$ (independent processing of each OFDM symbol). Conventional differential demodulation with $N = 2$. Iterative DF–DM with $N = 3, 5$ after four iterations.

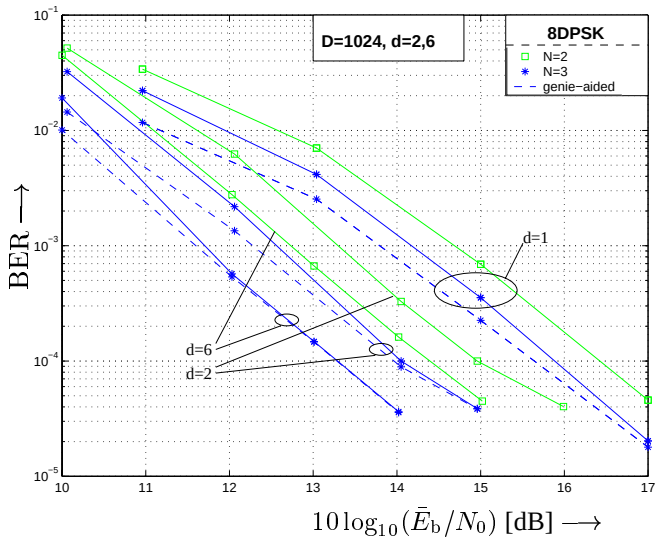

Fig. 6. BER over $10\log_{10}(\bar{E}_b/N_0)$. OFDM with $D = 1024$, 8DPSK, and diversity $d = 1, 2, 6$. Conventional differential demodulation with $N = 2$. Iterative DF–DM with $N = 3$ after four iterations.

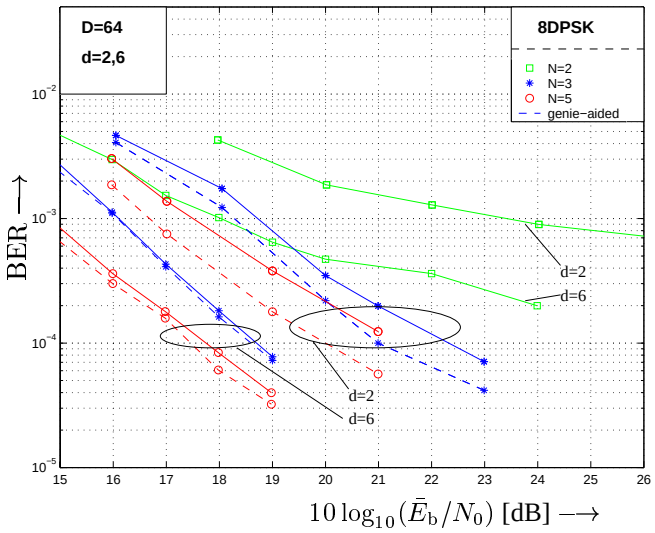

Fig. 8. BER over $10\log_{10}(\bar{E}_b/N_0)$. OFDM with $D = 64$, 8DPSK, and diversity $d = 2, 6$. Conventional differential demodulation with $N = 2$. Iterative DF–DM with $N = 3, 5$ after four iterations.